

Automatic Spiking Pulse-Coupled Neural Network for Image Segmentation

Jun Xi

Department of Math & Computer, Xinyu College, Xinyu, Jiangxi, China
94671326@qq.com

Abstract

Image segmentation is the process of partitioning a digital image into multiple segments with the purpose to simplify and/or change the representation of an image. The edges identified by edge detection are often disconnected. This paper introduces a 2-D Pulse-coupled neural network for the image segmentation. A new automatic spiking pulse-coupled neural network (SPCNN) parameters setting method is presented. The dynamic of the neuron and static characteristics of image could be connected so as to ensure the parameters of SPCNN. This approach does not need the training and experiments, which is very suitable for the real-time image processing. The experiments show the outperformances with Normalized Cuts approach. From the comparison, it could be observed that given the parameter V_L , if β is bigger, then the neuron in SPCNN model will be greater influenced by the neighboring neurons. That means in the space, there will be a bigger area which is formed by the neighboring neurons that can form a segmented sub-area. Additionally, α_e is bigger, then the precision of the SPCNN model will be lower. That indicates the segmented sub-areas will have wider gray range in the beginning iterations of SPCNN model.

Keywords: Image Segmentation, Neural Network, Pulse-coupled.

1. Introduction

Image segmentation is the process of partitioning a digital image into multiple segments with the purpose to simplify and/or change the representation of an image into something that is more meaningful and easier to analyze [1-2]. Image segmentation is typically used to locate objects and boundaries (lines, curves, *etc.*) in images [3]. More precisely, image segmentation is the process of assigning a label to every pixel in an image such that pixels with the same label share certain characteristics [4]. The result of image segmentation is a set of segments that collectively cover the entire image, or a set of contours extracted from the image. Each of the pixels in a region are similar with respect to some characteristic or computed property, such as color, intensity, or texture [5]. Adjacent regions are significantly different with respect to the same characteristic. When applied to a stack of images, typical in medical imaging, the resulting contours after image segmentation can be used to create 3D reconstructions with the help of interpolation algorithms like marching cubes [6].

Edge detection is a well-developed field on its own within image processing. Region boundaries and edges are closely related, since there is often a sharp adjustment in intensity at the region boundaries [7]. Edge detection techniques have therefore been used as the base of another segmentation technique. The edges identified by edge detection are often disconnected. To segment an object from an image however, one needs closed region boundaries. The desired edges are the boundaries between such objects or spatial-taxons which are information granules, consisting of a crisp pixel region, stationed at abstraction levels within a hierarchical nested scene architecture [8]. They are similar to

the Gestalt psychological designation of figure-ground, but are extended to include foreground, object groups, objects and salient object parts. Edge detection methods can be applied to the spatial-taxon region; in the same manner they would be applied to a silhouette [9]. This method is particularly useful when the disconnected edge is part of an illusory contour.

Segmentation methods can also be applied to edges obtained from edge detectors [10]. Lindeberg and Li developed an integrated method that segments edges into straight and curved edge segments for parts-based object recognition, based on a minimum description length (MDL) criterion that was optimized by a split-and-merge-like method with candidate breakpoints obtained from complementary junction cues to obtain more likely points at which to consider partitions into different segments [11]. Eckhorn proposed a neural network model which is based on a neuron working principle from a cat [12]. The model uses the coupling characteristics among different neighboring neurons. Thus, it is very suitable for image segmentation.

This paper introduces a 2-D Pulse-coupled neural network for the image segmentation. A new automatic spiking pulse-coupled neural network (SPCNN) parameters setting method is presented. The dynamic of the neuron and static characteristics of image could be connected so as to ensure the parameters of SPCNN. This approach does not need the training and experiments, which is very suitable for the real-time image processing.

The rest of this paper is organized following: section 2 presents the basic PCNN model and SPCNN model. Section 3 introduces the application of SPCNN in image segmentation.

2. Basic PCNN and SPCNN Model

PCNN is different from the traditional artificial neural network (ANN). PCNN has single layer with two dimensional structure, which is a 2-D matrix. The matrix relates to the pulse coupling neuron [12]. The other difference is PCNN does not need the training thus, the neuron is one-to-one associated to the image pixel.

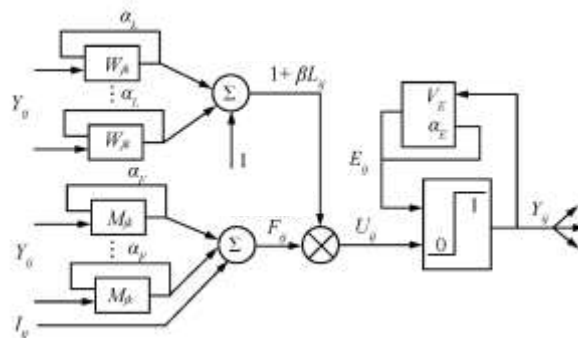


Figure 1. A Typical Single PCNN Model

From Figure 1, the basic PCNN model could be presented as:

$$F_{ij}(n) = e^{-\alpha_f} F_{ij}(n-1) + V_F \sum_{kl} M_{ijkl} Y_{kl}(n-1) + S_{ij} \quad (1)$$

$$L_{ij}(n) = e^{-\alpha_l} L_{ij}(n-1) + V_L \sum_{kl} W_{ijkl} Y_{kl}(n-1) \quad (2)$$

$$U_{ij}(n) = F_{ij}(n)(1 + \beta L_{ij}(n)) \quad (3)$$

$$Y_{ij}(n) = \begin{cases} 1 & \text{if } U_{ij}(n) > E_{ij}(n-1) \\ 0 & \text{else} \end{cases} \quad (4)$$

$$E_{ij}(n) = e^{-\alpha_e} E_{ij}(n-1) + V_E Y_{ij}(n) \quad (5)$$

There are two input in the location (i, j) of the neuron N_{ij} in the n iteration. They are feedback input F_{ij} and link input L_{ij} , which are connected by the neurons via weight matrix M and W with the 8 neighbors neurons. The previous input status is carried out by weights via the coefficient weakening factors $e^{-\alpha_f}$ and $e^{-\alpha_l}$. That indicates the influence of previous input on the current iteration input. Additionally, feedback input F_{ij} receives the output stimulation S_{ij} . After that, the two inputs generate the internal $U_{ij}(n)$ through the connect degree β . $U_{ij}(n)$ is compared with the previous dynamic threshold $E_{ij}(n)$ to determine if the N_{ij} is to be fired or not. If $U_{ij}(n) > E_{ij}(n)$, it is about to fire. If the neuron N_{ij} is fired, the dynamic threshold will be increased with the increasing of V_E . If the N_{ij} is not fired, the dynamic threshold will be weakened along with the coefficient factor $e^{-\alpha_e}$. Moreover, $Y_{ij}(n-1)$ presents the output of the previous neighbor's neuron. The parameters V_E , V_F , and V_L present the dynamic threshold value, feedback input value, and connect input value. The parameters α_e , α_l and α_f present the weakening coefficient factor of dynamic threshold E , connect input L , and feedback input F .

In this paper, a SCM simplified PCNN model is proposed. The SPCNN model could be expressed as:

$$U_{ij}(n) = e^{-\alpha_f} U_{ij}(n-1) + S_{ij}(1 + \beta V_L \sum_{kl} W_{ijkl} Y_{kl}(n-1)) \quad (6)$$

$$Y_{ij}(n) = \begin{cases} 1 & \text{if } U_{ij}(n) > E_{ij}(n-1) \\ 0 & \text{else} \end{cases} \quad (7)$$

$$E_{ij}(n) = e^{-\alpha_e} E_{ij}(n-1) + V_E Y_{ij}(n) \quad (8)$$

In this model, the fire condition is $U_{ij}(n) > E_{ij}(n-1)$. The internal activity $U_{ij}(n)$ is included two parts. $U_{ij}(n) = U_1 + U_2$. $U_1 = e^{-\alpha_f} U_{ij}(n-1)$ records the previous iterations of the neuron status through the coefficient weakening factor with sum weights. The second sub-item connect input is $L_{ij}(n) = V_L \sum_{kl} W_{ijkl} Y_{kl}(n-1)$ with a simplified feedback input: $F_{ij}(n) = S_{ij}$. Then, the non-linear generated result will be:

$$U_2 = F_{ij}(n)(1 + \beta L_{ij}(n)) = S_{ij}(1 + \beta V_L \sum_{kl} W_{ijkl} Y_{kl}(n-1)) \quad (9)$$

The main work will be focused on the five parameters: α_f , β , V_L , V_E , and α_e .

3. Parameters in SPCNN and Applications in Image Segmentation

3.1. Parameters in SPCNN

PCNN is widely used in the image processing [13]. The parameters play important roles in the application of SPCNN in image segmentation. General speaking, for different input images, the PCNN parameters could be adjusted by manual operations. Otherwise, they could be obtained from large number of training. This paper introduces a SPCNN parameter setting approach which is used in image segmentation. In this approach, the

dynamic characteristics will be associated with static image properties of each input image so as to determine the suitable parameters. The flow chart in Figure 2 is following the procedures.

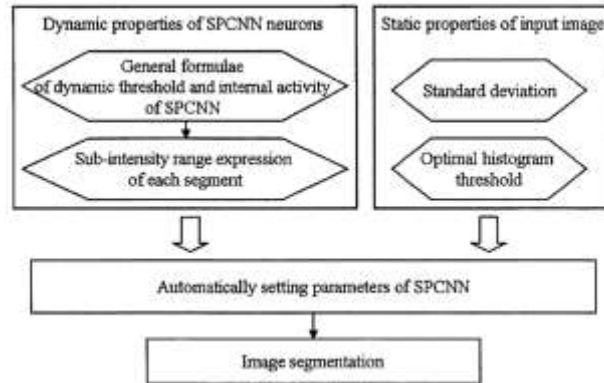


Figure 2. Flow Chart for SPCNN Parameter Setting

Figure 2 shows the flows of SPCNN parameter setting which is based on an automatically setting approach. There are several procedures. Firstly, the dynamic properties of SPCNN neurons include two aspects. One is general formulae of dynamic threshold and internal activity of SPCNN and the other is sub-intensity range expression of each segment. Secondly, the static properties of input image also include two aspects which are standard deviation and optimal histogram threshold. Thirdly, the previous two aspects determine the automatically setting parameters of SPCNN. Finally, the image segmentation will be based on the setting parameters of SPCNN.

The automatic spiking approach is able to set the parameters adjustable so as to control the image segmentation [14]. The aim is to achieve adaptive segmentation with improved parameter setting. Thus, we can get:

$$F_{ij}(n) = \sum_{kl \in N_{ij}} M_{ijkl} I_{kl} \quad (10)$$

$$L_{ij}(n) = \sum_{kl \in N_{ij}} W_{ijkl} Y_{kl}(n-1) \quad (11)$$

$$U_{ij}(n) = F_{ij}(n)[1 + \beta L_{ij}(n)] \quad (12)$$

$$Y_{ij}(n) = U_{ij}(n) > E_{ij}(n-1) \parallel Y_{ij}(n-1) \quad (13)$$

$$E_{ij}(n) = V_E H_\omega(F_{ij} - m_o(n)) \quad (14)$$

Where H_ω is a smooth step function which could be expressed by:

$$H_\omega(x) = \frac{1}{2} \left[1 + \frac{2}{\pi} \arctan\left(\frac{x}{\omega}\right) \right] \quad (15)$$

ω is the smooth degree when $x = 0$. In this approach, the neurons with high input density will be preferentially fired compared to the neurons with lower input density. That means pixels with high gray degree will have smaller fire cycle than the lower ones: $T_h < T_l$. Thus, the neurons with the lowest pixel value will be fired and they have the longest cycle called a pulsing cycle. Figure 3 shows the pulsing cycle and decay steps of the dynamic threshold. There are two neurons which include the two SPCNN models with the parallel behaviors. The two neurons have the same minimal non-zero gray input $s = 0.0039 \approx 1/255$. The parameters of the SPCNN will be automatically set as $\alpha_f = 0.2$, $\beta = 0.1$, $V_L = 1$, $\alpha_e = 0.7$ and $V_E = 10$.

The neurons' fire behaviors are based on the pulse cycle that is non-stop iteration. In each pulse cycle, each iteration associates the dynamic threshold weakening time [15]. Due to $T_h < T_l$, the neurons with high pixel values from an image will be more frequent than the lower pixel. Figure 4 presents the neuron activities within the first pulsing cycle.

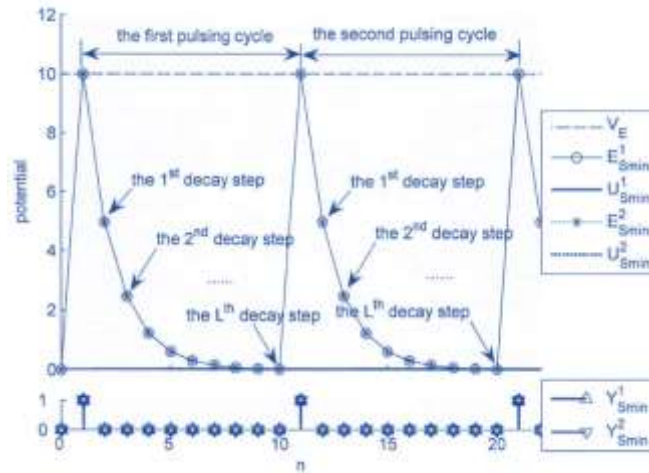


Figure 3. Two Neurons with Parallel Activities

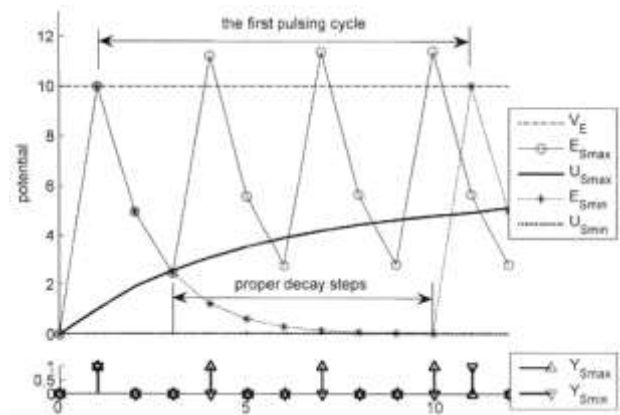


Figure 4. Maximal and Minimal Neural SPCNN Model Activities

Based on the Figure 3, in order to connect with the SPCNN model to process the images, the weight matrix will be:

$$W_{ijkl} = \begin{bmatrix} 0.5 & 1 & 0.5 \\ 1 & 0 & 1 \\ 0.5 & 1 & 0.5 \end{bmatrix} \quad (16)$$

From (6), the value of $\sum_{kl} W_{ijkl} Y_{kl}(n-1)$ will be changed along with the previous iterations of the eight neighbor neuron output with different group values. Assume that all the initial neuron statuses are $U[0]=0, Y[0]=0$, and $E[0]=0$. In the first iteration round, all the inputs of non-zero pixel value with internal activities and initial dynamic threshold meet the fire condition $U[1]=S > E[0]$. Thus, all the neurons will be fired in the first iteration $Y[1]=1$. If all the neuron associated pixel

are non-zero, the internal activities $\sum_{kl} W_{ijkl} Y_{kl}(1)$. The second iteration value is

$$\sum_{kl} W_{ijkl} Y_{kl}(1) = 6$$

$$U_{ij}[2] = U_{ij}[n_1 + 1] = S_{ij}(e^{-\alpha_f} + 1 + 6\beta V_L) = S_{ij}M[2] \quad (17)$$

Where $M[n]$ presents the n iterations. Internal activities of neuron input gray pixel value S . The dynamic threshold will be increased to V_E :

$$E_{ij}[1] = E_{ij}[n_1] = V_E \quad (18)$$

In the second iteration round, in order to confine the neurons will not be fired. The dynamic threshold value V_E is not smaller than the second iteration maximum pixel neuron internal activity value $U_{smax}[2] \leq E_{ij}[1] = V_E$.

$$E_{ij}[2] = E_{ij}[n_1 + 1] = V_E e^{-\alpha_e} \quad (19)$$

$$\begin{aligned} U_{ij}[3] &= U_{ij}[n_1 + 1 + 1] = e^{-\alpha_f} U_{ij}[2] + S_{ij}(1 + \beta V_L \sum_{kl} W_{ijkl} Y_{kl}[2]) \\ &= S_{ij}(e^{-\alpha_f} M[2] + 1) = S_{ij} \left(\frac{1 - e^{-3\alpha_f}}{1 - e^{-\alpha_f}} + 6\beta V_L e^{-\alpha_f} \right) = S_{ij}M[3] \end{aligned} \quad (20)$$

In the next iterations, the internal activities U_{ij} becomes more complex. It is not determined by the previous iteration value of internal activities, but also determined by the summary weight value of the neighbor neuron output. In the first pulse cycle, the dynamic threshold E_{ij} at weakening time l and the internal activity U_{ij} at the time $l+1$.

$$E_{ij}[n_1 + l] = V_E e^{-l\alpha_e} \quad (21)$$

$$\begin{aligned} U_{ij}[n_1 + 1 + l] &= e^{-\alpha_f} U_{ij}[n_1 + l] + S_{ij}(1 + \beta V_L \sum_{kl} W_{ijkl} Y_{kl}[n_1 + l]) \\ &= S_{ij}(e^{-\alpha_f} M[n_1 + l] + 1 + \beta V_L \sum_{kl} W_{ijkl} Y_{kl}[n_1 + l]) \\ &= S_{ij}(n_1 + l + 1) \end{aligned} \quad (22)$$

The neurons meet the fire condition: $U_{ij}(n_1 + l + 1) > E_{ij}(n_1 + l)$ will be fired at the weakening time $l+1$, then,

$$Y_{ij}(n_1 + l + 1) = 1 \quad (23)$$

The dynamic threshold will be increased at the weakening time $l+1$:

$$E_{ij}(n_1 + l + 1) = V_E (e^{-(l+1)\alpha_e} + 1) \quad (24)$$

At the later weakening time, the dynamic threshold will be weaken along with the coefficient $e^{-l\alpha_e}$.

3.2. Implementation in Image Segmentation

The SPCNN model is used in image segmentation with selecting several images for carrying out the experiments. The experiments are based on the platform which has Intel Core 2 Duo E8500 3.17 GHz. The Matlab 2009 is used for programming. For each image, SPCNN parameters could be achieved. In the image processing, in order to terminate the

SPCNN running, the ratio of fired neurons with total neurons is R . $R = \frac{Num_{fired}}{Num_{all}}$ where

Num_{fired} is the amount of fired neurons. Num_{all} is the total number of neurons.

If the value of R is bigger than a non-minus ε $R > \varepsilon$, $\varepsilon = (1/25)^2 = 0.0016$. That implies the size of the image captured by SPCNN. If $R \leq \varepsilon$, it implies the fired neurons are not enough during the iterations. There will be some discrete pixels or non-significant area. Thus, the SPCNN processing could be terminated. The unfired neurons will be put into the sub area. Therefore, ε should be suitable. Additionally, in the SPCNN iterations, when the amount of non-fired neurons is equal to the sum of the pixels with zero value, SPCNN iterations will be stopped. That because the gray value with zero will not be fired in SPCNN processing.

The SPCNN model is used for image segmentation. Each image will be processed with one second. In order to evaluate the SPCNN parameters automatic setting approach, the proposed model is compared with two image segmentation approaches. One is PCNN model with experienced values $\alpha_i = 1.0$, $\alpha_e = 1.0$, $\alpha_f = 0.1$, $V_F = 0.5$, $V_L = 0.2$, $V_E = 20$, and $\beta = 0.1$. The other one is Normalized Cuts approach.

From Figure 4, each row presents the segmentation results by using the proposed method comparing with Normalized Cuts approach. Nine images are selected for carrying out the experiments. The first column is the original image which will be processed in the experiments. The second, third, and fourth column is the output images with the parameters $n = 1, n = 2, n = 3$ of the SPCNN model which has the binary pulse output image. The column with a label is the processed images from the automatic parameters setting in the SPCNN model used for carrying out the image segmentation. Different colors are used for differentiate different segmented sub-areas, which indicates different targeted areas and scenarios. The b column indicate the images processed by the PCNN model with experienced values like $\alpha_i = 1.0, \alpha_e = 1.0, \alpha_f = 0.1, V_F = 0.5, V_L = 0.2, V_E = 20, \beta = 0.1$. The c column is the results from Normalized Cuts approach. For the first eight images, the best segmentation comes from the SPCNN model with automatic parameter setting. It could be observed that the targeted areas and background could be separated naturally by the curves. It results in significant sub-areas. While from the figures, the b column images with common experienced values, the targeted areas are not separated naturally due to the connection of both areas. That because the experienced values for PCNN can not present the characteristics of the image thus, it is not suitable for all the input images. While comparing with the Normalized Cuts approach, it is difficult to carry out the image segmentation except for the seventh image. It could be also found that, for the ninth image, all approaches are not able to identify the targeted areas like the animals and the trees that because the two areas have weak comparison from the pixels.

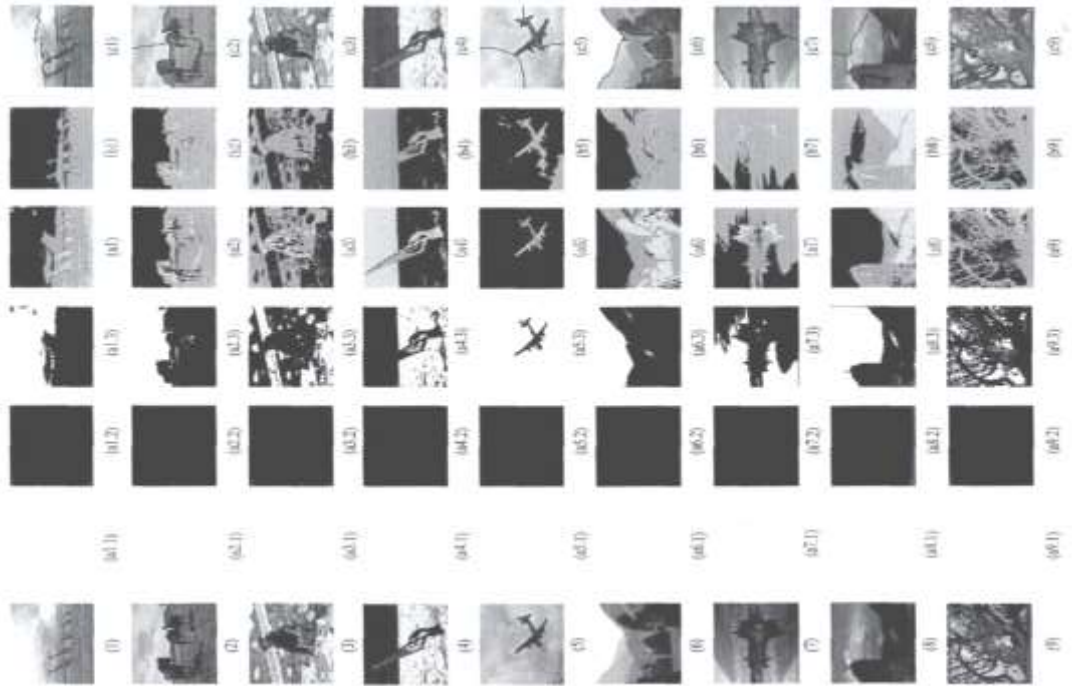


Figure 4. Experiment Results

Besides the images obtained from the experiments, table 1 presents the automatic setting parameters for the SPCNN model.

Table 1. Parameters for SPCNN Model

Exp. No.	V_L	β	α_f	V_E	α_e
1	1	0.072	1.472	1.662	0.544
2		0.145	1.386	2.125	0.956
3		0.104	1.431	1.863	0.739
4		0.126	1.044	2.110	0.756
5		0.364	1.951	3.329	1.974
6		0.109	1.243	1.944	0.724
7		0.267	1.749	2.775	1.583
8		0.440	1.600	3.844	2.065
9		0.176	1.540	2.270	1.144
1	0.352	0.204	1.472	1.662	0.544
2	0.950	0.153	1.386	2.125	0.956
3	0.444	0.233	1.431	1.863	0.739
4	0.615	0.205	1.044	2.110	0.756
5	0.138	2.625	1.951	3.329	1.974
6	0.057	1.888	1.243	1.944	0.724
7	0.813	0.328	1.749	2.775	1.583
8	0.202	2.172	1.600	3.844	2.065
9	0.381	0.461	1.540	2.270	1.144

By using the parameters from the table 1, the proposed SPCNN model with automatic setting parameters outperforms comparing with other approaches. The first column of Figure 4 is the natural gray image which will be input for the experiments. The second to fourth column images are the output processed by the proposed SPCNN model with three iterations. The fifth column is the SPCNN model with automatic parameter setting. The a.1 column is almost white pulse output image. That means all the non-zero pixels associated neurons are fired in the first iteration of SPCNN. The a.2 column is all black which means all the pixels are confined to be fired at the second iteration. The a.3 column presents the images each of which contains both white and black area. That implies in the third iteration, SPCNN is able to carry out the image segmentation into two areas. The white area is the first output from the image segmentation. The black part will be divided into smaller sub-areas along with the iterations in the SPCNN model.

From the comparison, it could be observed that given the parameter V_L , if β is bigger, then the neuron in SPCNN model will be greater influenced by the neighboring neurons. That means in the space, there will be a bigger area which is formed by the neighboring neurons that can form a segmented sub-area. Additionally, α_e is bigger, then the precision of the SPCNN model will be lower. That indicates the segmented sub-areas will have wider gray range in the beginning iterations of SPCNN model.

From the table, given the parameter $V_L = 1$, in the all experiments, β and α_e with the minimum value appears in the first image. It implies the first image should be segmented with smaller area so as to capture the neuron pixels with high precision. While the maximum values of β and α_e are in eighth image, this is opposite compared with the first image. Thus, it could be found that, the proposed SPCNN model with automatic parameter setting approach is able to adjust the suitable value according to the input image. Additionally, the proposed approach

can improve the segmentation efficiency. From the comparison of column, a , b , and c , it could be observed that column a is with the best effectiveness that because the SPCNN model using the automatically parameter setting. It is able to separate the targeted areas and background by natural curves.

4. Summary

This paper introduces a 2-D pulse-coupled neural network (SPCNN) approach according to different input images by using the adjustable automatic parameter setting method. This model is based on a SCM-enabled simplified PCNN. This proposed model is going to address the determination of suitable parameters by using manual or training-based methods which may cost lots of time. We build up a direct relation of the dynamic neurons and static image pixels. Based on the relations, the SPCNN model can adjust the parameters accordingly.

From this study, the dynamic characteristics of SPCNN model come from several aspects such as $U[n]$ distribution interval, dynamic threshold E_{ij} , and internal activity U_{ij} . While the static characteristics of the image pixels are the standard deviation and threshold of optimal column diagram. The relation enables the automatic parameter setting without any training and pre-definition. The experiments show the outperformances with Normalized Cuts approach.

The future research directions include several perspectives. Firstly, more characteristics from the input images could be selected for the experiments. The characteristics may include color information and veins features [16]. Secondly, the study will be extended by using the SPCNN model to deal with more complex images like GIS images. Thirdly, the parameters with more examples will be carried out for examining the precision of the output.

References

- [1] V. V. Kumar, N. G. Rao, and A. N. Rao, "RTL: reduced texture spectrum with lag value based image retrieval for medical images", *International Journal of Future Generation Communication and Networking*, vol. 2, (2009), pp. 39-48.
- [2] R. Y. Zhong, Q. Y. Dai, T. Qu, G. J. Hu and G. Q. Huang, "RFID-enabled Real-time Manufacturing Execution System for Mass-customization Production", *Robotics and Computer-Integrated Manufacturing*, vol. 29, (2013), pp. 283-292.
- [3] A. Kumar and S. Malhotra, "Pixel-Based Skin Color Classifier: A Review", *International Journal of Signal Processing, Image Processing and Pattern Recognition*, vol. 8, (2015), pp. 283-290.
- [4] R. Y. Zhong, Z. Li, A. L. Y. Pang, Y. Pan, T. Qu and G. Q. Huang, "RFID-enabled Real-time Advanced Planning and Scheduling Shell for Production Decision-making", *International Journal of Computer Integrated Manufacturing*, vol. 26, (2013), pp. 649-662.
- [5] R. Y. Zhong, G. Q. Huang, S. L. Lan, Q. Y. Dai, C. Xu and T. Zhang, "A Big Data Approach for Logistics Trajectory Discovery from RFID-enabled Production Data", *International Journal of Production Economics*, vol. 165, (2015), pp. 260-272.
- [6] Q. Y. Dai, R. Y. Zhong, G. Q. Huang, T. Qu, T. Zhang and T. Y. Luo, "Radio frequency identification-enabled real-time manufacturing execution system: a case study in an automotive part manufacturer", *International Journal of Computer Integrated Manufacturing*, vol. 25, no. 1, (2012), pp. 51-65.
- [7] X. Liu, X. Wang, N. Shi and C. Li, "Image Segmentation Algorithm Based on Improved Ant Colony Algorithm", *Journal of Convergence Information Technology*, vol. 8, no. 145, (2013).
- [8] Z. Fan, Q. Sun, Z. Ji, F. Ruan and L. Zhao, "An Image Filter Arithmetic based on GA, PDE and TV", *International Journal of Future Generation Communication and Networking*, vol. 6, (2013), pp. 147-156.
- [9] Y. Li and Y. Guo, "Gait Recognition Method Based on Lower Leg under 45 Degree Viewing Angle of Video", *International Journal of Future Generation Communication and Networking*, vol. 6, (2013), pp. 147-156.
- [10] J. Shi and J. Malik, "Normalized cuts and image segmentation", *Pattern Analysis and Machine Intelligence*, *IEEE Transactions on*, vol. 22, (2000), pp. 888-905.
- [11] P. F. Felzenszwalb and D. P. Huttenlocher, "Efficient graph-based image segmentation", *International Journal of Computer Vision*, vol. 59, (2004), pp. 167-181.

- [12] S. Zheng, M. M. Cheng, J. Warrell, P. Sturgess, V. Vineet and C. Rother, "Dense semantic image segmentation with objects and attributes", 2014 IEEE Conference on Computer Vision and Pattern Recognition (CVPR), (2014), pp. 3214-3221.
- [13] R. Y. Zhong, G. Q. Huang, S. Lan, Q. Dai, T. Zhang and C. Xu, "A two-level advanced production planning and scheduling model for RFID-enabled ubiquitous manufacturing", *Advanced Engineering Informatics*, vol. 29, (2015), pp. 799-812.
- [14] L. Y. Pang, Z. Li, G. Q. Huang, R. Y. Zhong, Y. Pan and T. Qu, "Reconfigurable Auto-ID Enabled Software as a Service (SaaS) Shell for Real-Time Fleet Management in Industrial Parks", *Journal of Computing in Civil Engineering*, 10.1061/(ASCE)CP.1943-5487.0000306, 04014032, (2014).
- [15] B. Cai, Z. Liu, J. Wang and Y. Zhu, "Image Segmentation Framework Using Gradient Guided Active Contours", *International Journal of Signal Processing, Image Processing and Pattern Recognition*, vol. 8, (2015), pp. 51-62.
- [16] R. Y. Zhong, S. T. Newman, G. Q. Huang and S. Lan, "Big Data for supply chain management in the service and manufacturing sectors: Challenges, opportunities, and future perspectives", *Computers & Industrial Engineering*, doi:10.1016/j.cie.2016.07.013, (2016).

Author

Xi Jun, he is currently a lecturer from Department of Math & Computer, Xinyu College. He graduated from East China Normal University with master degree of software engineering. His research interests include Image Processing, Computer Network and Security, as well as Database Technologies. He has published over 10 papers in international journals and conferences.

